View Article Online
DOI: 10.1039/C8CE01580E

Modulation of coordination in pincer-type isonicotinohydrazone Schiff base ligands by proton transfer

Ghodrat Mahmoudi[a]*, Ali Akbar Khandar[b], Farhad Akbari Afkhami[b], Barbara Miroslaw[c], Atash V. Gurbanov[d,e], Fedor I. Zubkov[f], Alan Kennedy[g], Antonio Franconetti[h] and Antonio Frontera[h,*]

[a]*Department of Chemistry, Faculty of Science, University of Maragheh, P.O. Box 55181-83111, Maragheh, Iran*

[b]*Department of Inorganic Chemistry, Faculty of Chemistry, University of Tabriz, P.O. Box 5166616471 ,Tabriz, Iran*

[c]*Department of Crystallography, Faculty of Chemistry, Maria Curie-Sklodowska University,*

Pl. Marii Curie-Sklodowskiej 3, 20-031 Lublin, Poland barbara.miroslaw@poczta.umcs.lublin.pl

[d]*Department of Organic Chemistry, Baku State University, Z. Khalilov str. 23, AZ 1148, Baku, Azerbaijan*

[e]*Centro de Química Estrutural, Instituto Superior Técnico, Universidade de Lisboa, Av. Rovisco Pais, 1049–001 Lisboa, Portugal*

[f]*Organic Chemistry Department, Faculty of Science, Peoples' Friendship University of Russia (RUDN University), 6 Miklukho-Maklaya St., Moscow, 117198, Russian Federation*

[g]*Department of Pure & Applied Chemistry, University of Strathclyde, 295 Cathedral Street, Glasgow G1 1XL, Scotland, UK*

[h]*Departament de Química, Universitat de les Illes Balears, Crta. de Valldemossa km 7.5, 07122 Palma de Mallorca (Baleares), SPAIN*

Published on 30 October 2018. Downloaded by University of Strathclyde on 10/31/2018 6:29:35 PM.

CrystEngComm Accepted Manuscript

View Article Online
DOI: 10.1039/C8CE01580E

Published on 30 October 2018. Downloaded by University of Strathclyde on 10/31/2018 6:29:35 PM.

Abstract

We present here two different coordination polyhedra of pincer type N_2O hydrazone based ligands supplemented with thiocyanate ions. The compounds namely $[Hg(SCN)_2(HL^1)]$ (**1**) and $[Hg(SCN)_2(HL^2)]$ (**2**) have a common isonicotinohydrazone fragment and have been prepared by using a coordination driven self-assembly of the $Hg(SCN)_2$ with two different ligands including 2-benzoylpyridine-isonicotinoylhydrazone (HL^1), and 2-acetylpyridine-isonicotinoylhydrazone (HL^2). In compound **1** the ligand coordinated to the mercury center in the keto form (=N–NH=C=O) whereas, in compound **2**, the proton at the hydrazine group have been shifted to the uncoordinated pyridine ring and the ligand acted as a zwitterion. The structures provide a complementary system for proton transfer within the ligand molecule involving the keto-enol tautomerization of amide group and 4-pyridyl N protonation. As a result, the relative location of orbitals and ligands in the complexes are different as well as the bonding strength and the coordination polyhedra. We have also studied electrostatically enhanced $\pi\cdots\pi$ (either conventional or involving the chelate ring) interactions observed in the solid state of both compounds and analyzed them using DFT calculations, Molecular Electrostatic Potential surface and the Bader's theory of atoms in molecules.

CrystEngComm Accepted Manuscript

View Article Online
DOI: 10.1039/C8CE01580E

Published on 30 October 2018. Downloaded by University of Strathclyde on 10/31/2018 6:29:35 PM.

Introduction

The crystal engineering is not a trivial problem and still many aspects of controlling crystal growth need to be studied and it is not easy to predict the outcome of crystallization.[1-6] In fact, a major challenge using polydentate chelating-bridging building blocks in the synthesis of metal coordination compounds is the unpredictability of the structure of the products which may depend on several factors such as the nature of the ligands used, the oxidation state, geometry, and size of the metal centers, the metal-to-ligand ratio, etc.[7-9] Hydrazone-pyridine based chelating ligands are known N,N,O pincer type ligands.[10] They are usually synthesized by the one-pot Schiff-base condensation reaction in high yields[11] and it makes them a good subject for studies because the geometries of the ligands can have a great impact on the structural architecture of coordination compounds.[12] Pyridine based ligands containing amide groups generally are coordinated to the metal centers through their pyridyl nitrogen atoms and interact with each other by hydrogen bonds involving the amide groups, and the location of pyridyl substituent at peripheral part of the main molecular skeleton in the isonicotinohydrazone based ligand may result in interesting supramolecular motifs.[13] The chromophore hydrazone functional group is conformationally flexible and it has numerous hydrogen bonding sites including a molecular backbone. Moreover, isonicotinohydrazone based ligand possesses an additional pyridine hydrogen bond acceptor region and the ability to establish π···π stacking interactions taking advantage of the aromatic rings located on the two extremities of the molecule.[13] The strength of coordination bonding may, however, be tuned by some changes in electronic structure of the ligand when proton transfer occurs (Scheme 1). In pyridyl groups the electron lone pair does not delocalize, therefore it is a good proton acceptor. On the other hand, the amide part may undergo keto-enol transformation.[14] By tuning the crystallization conditions, the resulting complexes may have different localization of proton within the ligand molecule and different coordination architecture.[13c,14f] In the present work we study the differences in structure of two mercury(II) coordination compounds of hydrazone Schiff bases containing pyridine groups. The change in electronic structure of ligand, due to the proton transfer, changes its ligating properties and the relative location of orbitals and ligands.

CrystEngComm Accepted Manuscript

View Article Online
DOI: 10.1039/C8CE01580E

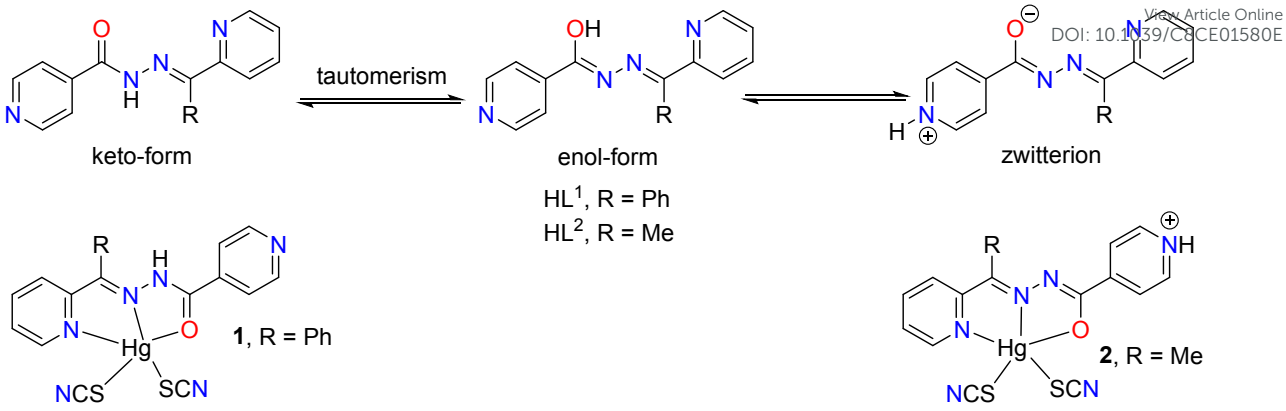

Scheme 1. Possible proton transfer mechanisms in isonicotinohydrazone based ligands and the structure of complexes **1** and **2**

The geometric features and the coordination behavior of the ligands in the crystal structure of compound **2** revealed a preference for the formation of a chelate ring stacking along with more conventional pyridine···pyridine stacking interactions. In contrast, the steric effect of phenyl group in HL^1 ligand (compound **1**) prevents the formation of chelate ring stacking. To gain insight into these structural features, we employed Hirshfeld surface analysis and DFT (M06-2X) calculations of interaction energies, which confirm that chelate ring stacking is a robust synthon to be considered in crystal engineering.

Experimental and theoretical methods

Materials and methods

All chemicals were commercially available and the solvents used without further purification. The hydrazone-pyridine based ligands were synthesized according to the reported method as described elsewhere.[8] In short, pure HL^1 and HL^2 were obtained by the condensation of ethanolic solutions of isonicotinohydrazide, and 2-benzoylpyridine and 2-acetylpyridine respectively. Elemental analyses were carried out using a Heraeus CHN-O-Rapid analyzer and FT-IR spectra were recorded on a Bruker Tensor 27 FT-IR spectrometer with KBr pellets in the range of 4000–400 cm^{-1}. Melting points of the prepared metal complexes were measured using an Electrothermal 9100 apparatus.

Synthesis of the complexes

Compounds $[Hg(SCN)_2(HL^1)]$ (**1**) and $[Hg(SCN)_2(HL^2)]$ (**2**) were synthesized using the same method mixing equimolar quantities of mercury(II) salt and ligand, as explained below. A

Published on 30 October 2018. Downloaded by University of Strathclyde on 10/31/2018 6:29:35 PM.

CrystEngComm Accepted Manuscript

View Article Online
DOI: 10.1039/C8CE01580E

branched tube was used to obtain suitable crystals for X-ray determination, as detailed in Scheme S1.

$[Hg(SCN)_2(HL^1)]$ (1). Mercury (II) thiocyanate (0.158 g, 0.5 mmol) and 2-benzoylpyridine-isonicotinoylhydrazone (HL^1) (0.113 g, 0.5 mmol) were placed in the main arm of a branched tube. Methano l(10 ml) was carefully added to fill the arms. The tube was sealed and immersed in an oil bath at 60°C while the branched arm was kept at ambient temperature. After 3 days, crystals of **1** that isolated in the cooler arm were filtered off, washed with acetone and ether, and dried in air. The isolated yield was 0.217 g, 70%. m. p. 206 ºC. Anal. Calcd for $C_{20}H_{14}HgN_6OS_2$: C, 38.80; H, 2.28; N, 13.57%. Fund: C, 38.49H, 2.17; N, 13.94%. FT-IR (cm^{-1}) selected bands: 3452 (w), 3093(w), 2117(vs), 1663(m), 1596 (m), 1538(vs), 1466 (m), 1437 (m), 1282 (vs), 1136 (m), 965 (m), 839 (m), 772 (m) and 661 (m).

$[Hg(SCN)_2(HL^2)]$ (2). Mercury (II) thiocyanate (0.158 g, 0.5 mmol) and 2-acetylpyridine-isonicotinoyl hydrazone (HL^2) (0.120 g, 0.5 mmol) were placed in the main arm of a branched tube. Methanol(10 ml) was carefully added to fill the arms. The tube was sealed and immersed in an oil bath at 60°C while the branched arm was kept at ambient temperature. After 3 days, crystals of **2** that isolated in the cooler arm were filtered off, washed with acetone and ether, and dried in air. The isolated yield was 0.240 g, 84%. m. p. 180 ºC. Anal. Calcd for $C_{15}H_{12}HgN_6OS_2$: C, 32.34; H, 2.17; N, 15.09%. Fund: C, 32.60; H, 2.22; N, 15.29%. FT-IR (cm^{-1}) selected bands: 3423(w), 3368(w), 2993 (w), 2061(vs), 1622(m), 1593 (m), 1534(s), 1481 (s), 1438 (m), 1288 (s), 1157 (m), 948 (m), 834 (m), 787 (m) and 699 (m).

Hirshfeld surface analysis

The Hirshfeld surfaces and 2D fingerprints of studied compounds were generated with the use of the Crystal Explorer package ver. 3.1.[15] Crystal structures were imported from CIF files. Hirshfeld surfaces were generated using high resolution and mapped with the d_{norm} and shape-index functions. 2D fingerprint plots were prepared with the use of the same software.

X-ray diffraction

The diffraction intensities for **1** and **2** were measured at room by the ω-scan technique on Bruker four-circle diffractometers (APEX-II CCD with graphite-monochromated MoKα radiation (λ=0.71073 Å). The detector frames were integrated by use of the program SAINT[16] and the empirical absorption corrections were performed using SADABS program.[17] The structures were solved and refined using SHELXS and olex2.refine refinement package using

Published on 30 October 2018. Downloaded by University of Strathclyde on 10/31/2018 6:29:35 PM.

CrystEngComm Accepted Manuscript

View Article Online
DOI: 10.1039/C8CE01580E

Gauss-Newton minimization.[18,19] All non-hydrogen atoms were refined anisotropically, positions of all hydrogen atoms were placed in idealized positions except of H atom at pyridine in **2** which was found in the difference Fourier maps. Then all H-atoms were refined as 'riding model' with isotropic displacement parameters set at 1.2 (1.5 for methyl groups) times U_{eq} of appropriate carrier atoms. Details of crystallographic data collection and refinement parameters are given in Table 1.

CCDC 1867818-1867819 contain the supplementary crystallographic data for this paper. These data can be obtained free of charge via http://www.ccdc.cam.ac.uk/conts/retrieving.html (or from the Cambridge Crystallographic Data Centre, 12, Union Road, Cambridge CB2 1EZ, UK; fax: +44 1223 336033).

Theoretical Methods

The geometries of the complexes included in this study were computed at the M06-2X/def2-TZVP level of theory using the crystallographic coordinates within the GAUSSIAN-09 program.[20] For the Hg atom we have used the LanL2DZ basis set. This level of theory is adequate for studying noncovalent interactions dominated by dispersion effects like π-stacking. The basis set superposition error for the calculation of interaction energies has been corrected using the counterpoise method.[21] The "atoms-in-molecules" (AIM)[22] analysis of the electron density has been performed at the same level of theory using the AIMAll program.[23] Molecular Electrostatic Potential surfaces have been computed at the same level using the GAUSSIAN-09 program.

Results and discussion

Molecular structure

Compound **1** crystallizes in the monoclinic *C*2/*c* space group (Table 1) with the amide fragment being in a keto tautomeric form. A voluminous benzyl group is substituted at C7 atom and it is rotated by *ca*. 60° in regard to the hydrazone mean plane (Fig. 1). Compound **2** ($P2_1/c$) has a methyl substituent instead of benzyl one. Under the reaction condition, the amide group undergoes the deprotonation. The proton is transferred form amide N1 to pyridyl N4 atom forming a zwitterion (Fig. 2). The bond lengths (Table 2), as well as intermolecular hydrogen bond motives (Table S1, Figs S1-S2), confirm the keto form in **1** and the enol form of the amide group in **2**. The C1–N1 bond length in **2** is shorter by 0.02 Å, whereas the C1–O1 and C1–C8 bonds are longer by 0.03 and 0.02 Å, respectively, than in the keto form in **1**. The electronic

Published on 30 October 2018. Downloaded by University of Strathclyde on 10/31/2018 6:29:35 PM.

CrystEngComm Accepted Manuscript

View Article Online
DOI: 10.1039/C8CE01580E

coupling in molecule in crystal **2** results in a flat structure (Table 3 and Fig 3). Conversely, in compound **1** the molecule is bent where the hydrazone fragment is not planar with O1 and C8 atoms being below (0.21 Å) and above (0.30 Å) the mean C1N2N1 plane, respectively. A comparison of both compounds is provided in Fig. 3.

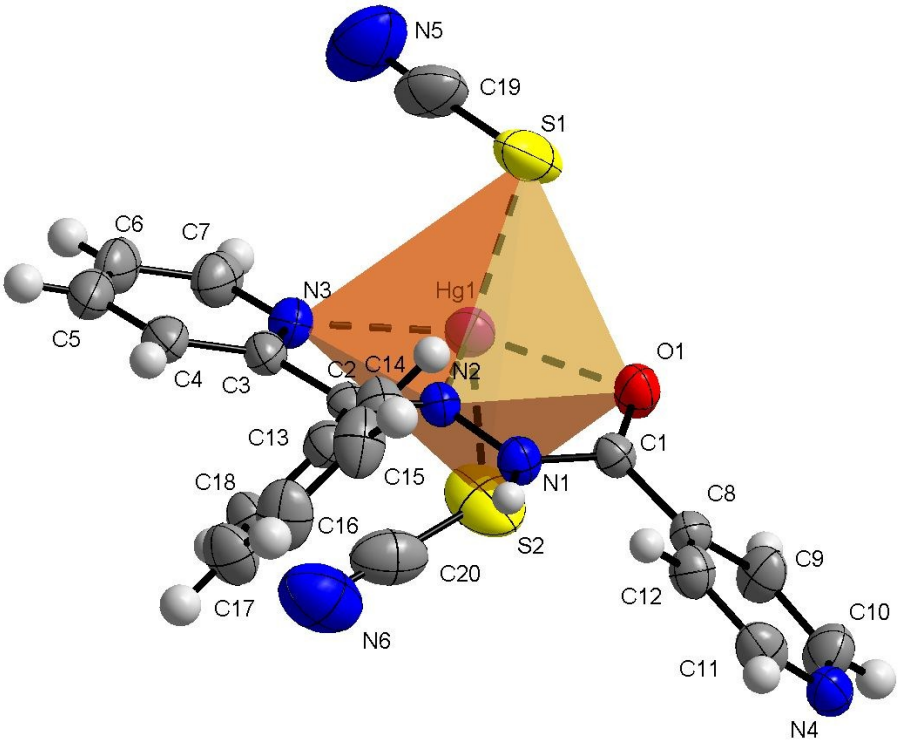

Fig. 1. Thermal ellipsoids and coordination polyhedron in **1**.

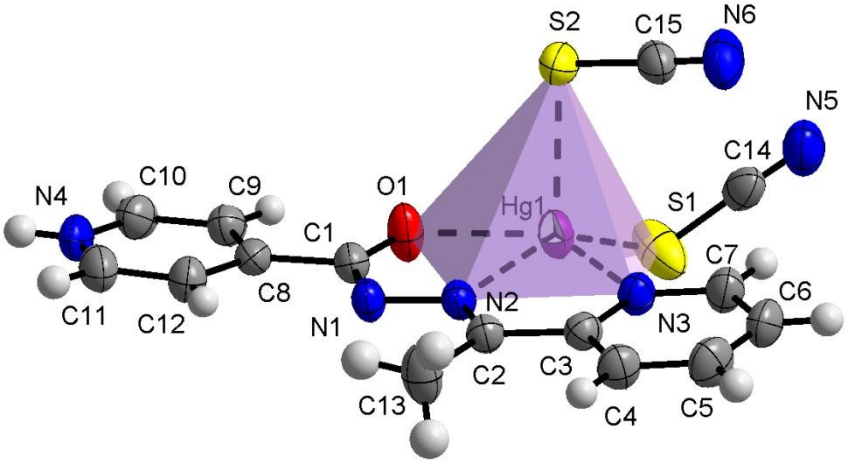

Fig. 2. Thermal ellipsoids and coordination polyhedron in **2**.

Published on 30 October 2018. Downloaded by University of Strathclyde on 10/31/2018 6:29:35 PM.

CrystEngComm Accepted Manuscript

View Article Online
DOI: 10.1039/C8CE01580E

Table 1. Crystal data and structure refinement data for **1** and **2**.

Crystal	**1**	**2**
Empirical formula	$C_{20}H_{14}N_6OS_2Hg$	$C_{15}H_{12}N_6OS_2Hg$
Formula weight	619.11	557.04
Temperature/K	296(2)	296(2)
Crystal system	monoclinic	monoclinic
Space group	*C*2/*c*	$P2_1/c$
a/Å	28.861(6)	12.9176(3)
b/Å	9.191(2)	7.7756(2)
c/Å	17.149(3)	17.4321(4)
β/°	111.76(3)	93.02(1)
Volume/Å^3	4224.8(17)	1748.5(1)
Z	8	4
ρ_{calc}g/cm^3	1.9465	2.1159
μ/mm^{-1}	7.510	9.060
F(000)	2353.2	1048.6
Crystal size/mm^3	0.20 × 0.22 × 0.40	0.08 × 0.22 × 0.24
Radiation	Mo Kα (λ = 0.71073)	Mo Kα (λ = 0.71073)
2Θ range for data collection/°	4.68 to 50.48	3.16 to 65.12
Reflections collected	11606	40853
	3711	6334
Independent reflections	R_{int} = 0.0433,	R_{int} = 0.0285,
	R_{sigma} = 0.0483	R_{sigma} = 0.0248
Data/restraints/parameters	3711/0/270	6334/0/226
Goodness-of-fit on F^2	0.829	0.990
Final R indexes [I>=2σ (I)]	R_1 = 0.0366, wR_2 = 0.0830	R_1 = 0.0256, wR_2 = 0.0441
Final R indexes [all data]	R_1 = 0.0561, wR_2 = 0.0880	R_1 = 0.0460, wR_2 = 0.0497
Largest diff. peak/hole / e Å^{-3}	1.85/-2.35	1.32/-1.55
CCDC No.	1867818	1867819

Published on 30 October 2018. Downloaded by University of Strathclyde on 10/31/2018 6:29:35 PM.

CrystEngComm Accepted Manuscript

View Article Online
DOI: 10.1039/C8CE01580E

The consequences of proton transfer are also pronounced in the geometry of the coordination spheres. In both complexes the organic ligands serve as tridentate N_2O pincer type chelator, but in the zwitterionic structure **2** the distance between Hg1···O1 atoms is shorter (by 0.29 Å) than in **1** (Table 2). Additionally, the ligand to metal orbital relative orientation is different. In **1** the coordination polyhedron is a deformed trigonal bipyramid (Fig. 1). The pincer ligand lies in the base and two thiocyanate ions are in the apical positions at nearly the same distance of *ca*. 2.4 Å. In **2** the pincer ligand is bonded stronger to the metal center with shorter intramolecular N–Hg and O–Hg distances than in **1**. It forms a distorted square pyramid with isonicotinohydrazone part of the ligand and with one of the SCN^- ions lying in the same plane. The second thiocyanate anion takes the apical position with longer distance Hg1–S2 of 2.640(1) Å (Fig. 2).

Table 2. Selected bond lengths for **1** and **2** in Å.

Bond	1	2	Bond	1	2
Hg1–N2	2.491(5)	2.279(2)	C7–N3	1.334(9)	1.332(4)
Hg1–N3	2.423(6)	2.459(2)	C8–C9	1.371(10)	1.389(4)
Hg1–S1	2.399(2)	2.428(1)	C8–C12	1.380(10)	1.385(4)
Hg1–S2	2.406(2)	2.640(1)	C9–C10	1.385(10)	1.372(4)
Hg1–O1	2.687(5)	2.392(2)	C10–N4	1.312(10)	1.324(4)
C1–O1	1.226(7)	1.257(3)	C11–N4	1.342(10)	1.327(4)
C1–N1	1.346(9)	1.324(3)	C11–C12	1.377(10)	1.373(4)
C1–C8	1.477(9)	1.499(4)	N5–C19/ or C14	1.143(13)	1.143(4)
N1–N2	1.382(7)	1.372(3)	N6–C20/ or C15	1.158(14)	1.148(4)
N2–C2	1.282(9)	1.288(3)	S1–C19/ or C14	1.643(11)	1.667(4)
C2–C13	1.467(9)	1.496(4)	S2–C20/ or C15	1.650(13)	1.649(3)
C3–N3	1.346(9)	1.338(3)			

Table 3. Selected bond angles and torsions in **1** and **2** in deg.

Angle	1	2
S1–Hg1–S2	152.1(1)	107.5(1)
O1–Hg1–S1	86.1(1)	108.6(1)
O1–Hg1–S2	85.5(1)	96.3(1)
N2–Hg1–O1	61.8(2)	69.1(1)
N3–Hg1–O1	126.7(2)	138.0(1)
S1–Hg1–N2	104.6(1)	148.8(1)
S1–Hg1–N3	101.4(1)	105.5(1)
S2–Hg1–N2	94.7(1)	103.6(1)
S2–Hg1–N3	105.0(2)	96.1(1)
N2–Hg1–N3	65.4(2)	69.0(1)

Published on 30 October 2018. Downloaded by University of Strathclyde on 10/31/2018 6:29:35 PM.

CrystEngComm Accepted Manuscript

View Article Online
DOI: 10.1039/C8CE01580E

Hg1–S1–C19/ or C14	100.2(4)	97.6(1)
Hg1–S2–C20/ or C15	96.7(3)	99.7(1)
O1–Hg1–N3–C7	171.1(5)	175.9(2)
C1–N1–N2–Hg1	13.2(7)	2.6(3)
N1–N2–Hg1–N3	169.0(5)	179.0(2)

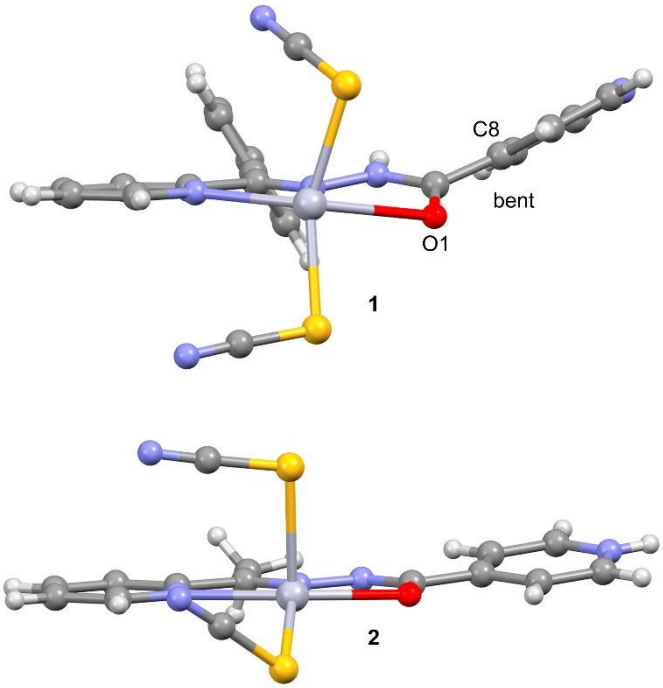

Fig. 3. Comparison of the planarity of the ligands in complexes of **1** (top) and **2** (bottom).

π···π interactions

The flattening of isonicotinohydrazone moiety in **2** is essential for π···π intermolecular interactions. In **2** the 2-pyridyl and 4-pyridyl rings (R1 and R2 in Table S2) interact to each other with nearly full molecular overlay (Fig. 4, Table S2). In **1** the π…π interaction is possible only between two 2-pyridyl fragments of the molecules transformed by inversion (R1 rings in Table S2; Fig. 5). The second π···π contact in **1** is between 4-pyridyl and benzyl rings (R2 and R3 in Table S2). In crystal of **2** the columns of stacked molecules are the main packing motif. Whereas in **1** a zig-zag arrangement is present.

Published on 30 October 2018. Downloaded by University of Strathclyde on 10/31/2018 6:29:35 PM.

CrystEngComm Accepted Manuscript

View Article Online
DOI: 10.1039/C8CE01580E

Published on 30 October 2018. Downloaded by University of Strathclyde on 10/31/2018 6:29:35 PM.

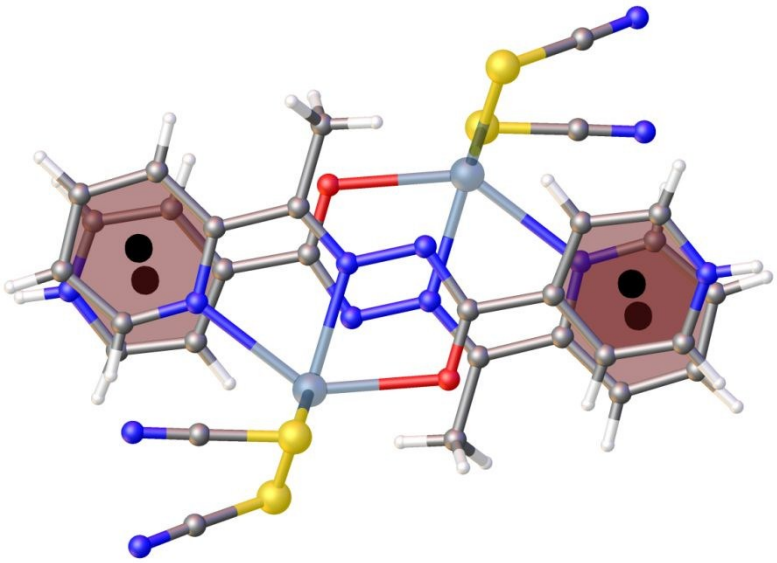

Fig. 4. The π···π intermolecular interactions between 2- pyridyl and 4-pyridyl rings in **2** (nearly full overlay of the molecules).

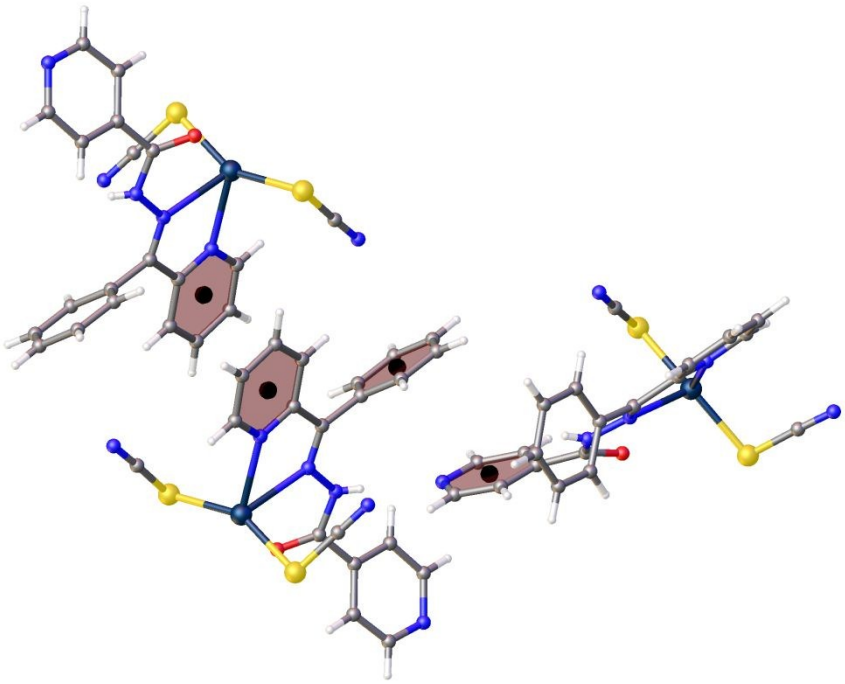

Fig. 5. The π···π intermolecular interactions between two 2-pyridyl rings and between 4-pyridyl and benzyl rings in **1**.

CrystEngComm Accepted Manuscript

View Article Online
DOI: 10.1039/C8CE01580E

Published on 30 October 2018. Downloaded by University of Strathclyde on 10/31/2018 6:29:35 PM.

IR spectroscopy

The IR spectrum of **1**, where the amide N-atom is not deprotonated, exhibits both the amide N-H (3452 cm^{-1}) and C=O (1663 cm^{-1}) stretching vibrations that are typical for a free ligand[24] and there is no peak characteristic of the deprotonated ligand. On the other hand, the free ligand C=O stretching vibrations is not observed in the IR spectrum of compound **2** and an absorption band response to the C=N–N=C–O moiety appeared around 1622 cm^{-1} indicates that the ligand has lost the amide proton during the tautomerization, and the proton is attached to the pyridyl nitrogen of the isonicotine fragment making a zwitterion.

Hirshfeld surface analysis

The Hirshfeld surface analysis[25,26] of **1** and **2** gives a clear difference in molecular structure and crystal packing. The antennas related to N…H contacts in **2** are longer and narrower than in **1** as a result of shorter N···H intermolecular interactions in **2** (Fig. 6). In **1** the additional aromatic substituent cause that the H···H contacts are more abundant (21.3 *vs* 13.7%), but the aromatic character of the molecule is more pronounced in N…N contacts due to π···π stacks in **2** (0.9 vs 0.1%). The Hg···H contacts show that in **2** the metal core is more hindered than in **1** (0.2 vs 1.2%).

CrystEngComm Accepted Manuscript

View Article Online
DOI: 10.1039/C8CE01580E

Published on 30 October 2018. Downloaded by University of Strathclyde on 10/31/2018 6:29:35 PM.

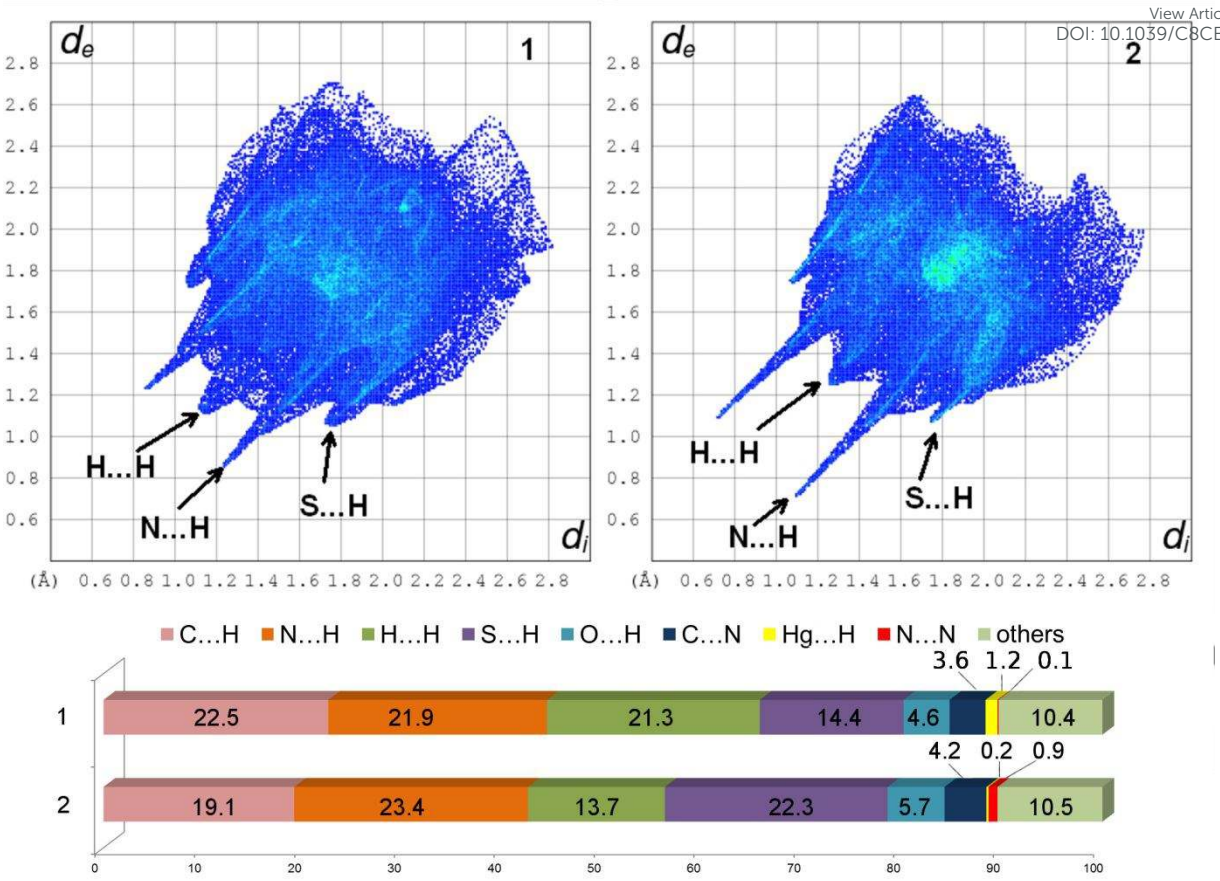

Fig. 6. 2D fingerprint plots and percentage contributions of contacts to the Hirshfeld surface in the structures of **1** and **2** calculated from crystal structures.

Theoretical study

The theoretical study reported herein is devoted to compare the energetic features of the two types of π-stacking interactions (chelate ring–π and π–π) observed in the crystal packing of compounds **1**–**2** described above (see Figs. 4 and 5). These interactions are crucial to understanding the crystal packing of complexes **1**–**2**. In addition to the classical π-stacking interaction involving aromatic rings, other planar moieties can also participate in more "unconventional" stacking interactions.[27] For instance, chelate rings with delocalized π bonds establish stacking[27] interactions similar to those of aromatic organic molecules[28] in transition-metal complexes. Similar chelate ring π-stacking interactions have been also reported by us in HgX_2 and PbX_2 (X = Cl, Br and I) coordination compounds.[13-14]

To study the donor-acceptor ability of HgL_n complexes, we have computed the molecular electrostatic potential (MEP) surfaces of compounds **1** and **2**, which are shown in Fig. 7. Expectedly, the most negative electrostatic potential corresponds to the region of the SCN

CrystEngComm Accepted Manuscript

View Article Online
DOI: 10.1039/C8CE01580E

ligands and the most positive part is located in the region of the N–H groups. Therefore, H-bonding interaction between the N–H and SCN groups should be energetically favored. Furthermore, perpendicularly to the molecular plane, in compound **2** each 5-membered chelate ring has almost negligible MEP values. Consequently, the stacking interactions between chelate rings will be likely dominated by dispersion effects. The MEP value is large and positive over the protonated pyridine rings and it is negative (–5 kcal/mol) in the coordinated pyridine ring. Therefore, pyridine–pyridine interactions are expected to be electrostatically very favored due to a significant electrostatic attraction. In compound **1**, the chelate ring are not accessible to the particular geometry around the Hg metal center and the location of the SCN ligands.

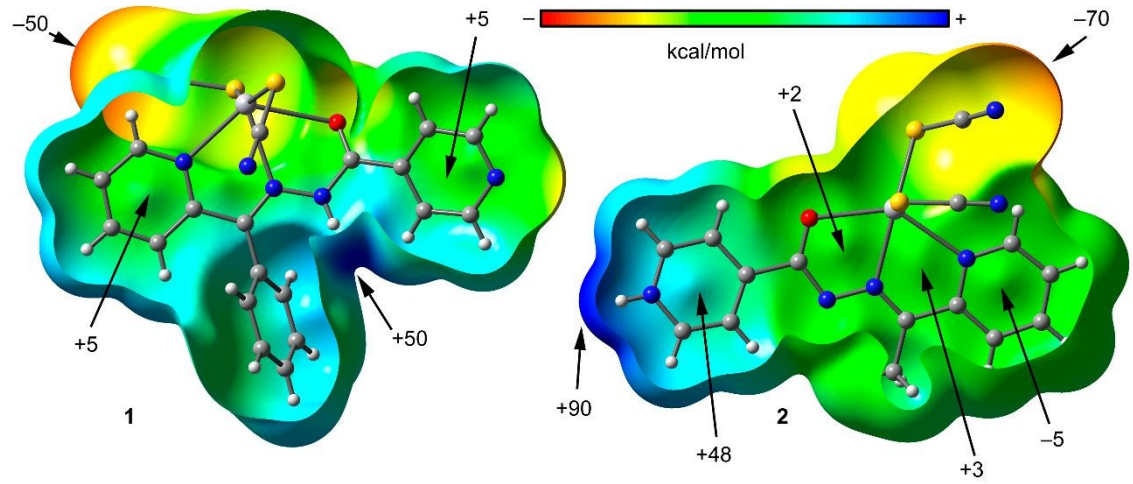

Fig 7. MEP surfaces plotted onto the van der Waals surfaces of compound **1** (left) and **2** (right) The energies at selected points of the surface are given in kcal/mol.

In the crystal packing of compounds **1**, the mononuclear Hg(II) complex forms self-assembled dimers in the solid state governed by the formation of an antiparallel π–π interactions involving the coordinated pyridine rings, assisted by H-bonding interactions between the aromatic CH bonds and the pseudohalide (see Fig. 8a). These CH···N/S hydrogen bonds are expected to be energetically strong due to the enhanced acidity of the H atoms due to the coordination of the pyridide to the Hg(II) metal center. The dimerization energy of this self-assembled dimer is ΔE_1 = –27.9 kcal/mol, which is large due to the contribution of both interactions. In an effort to calculate the contribution of the different, we have computed a theoretical model in which one of the pseudoligands (SCN^-) has been replaced by a hydrido ligand (see small arrows in Fig. 8b) and consequently the H-bonding interactions are not formed. Consequently, the interaction energy is reduced to ΔE_2 = –15.9 kcal/mol that can be attributed to the contribution of the antiparallel π-stacking interaction. This binding energy is stronger than more conventional π-

Published on 30 October 2018. Downloaded by University of Strathclyde on 10/31/2018 6:29:35 PM.

CrystEngComm Accepted Manuscript

View Article Online
DOI: 10.1039/C8CE01580E

stacking interactions[27] due to the presence of the Hg(II) metal center that increases considerably the dipole moment of the π-system. The contribution of the H-bonding interactions to the formation of the assembly can be evaluated by difference ($\Delta E_1 - \Delta E_2$ = –12.0 kcal/mol), thus revealing a major contribution of the π-stacking.

In order to provide additional evidence for the existence of the noncovalent interactions commented above we have analyzed the self-assembled π-stacked dimer of compound **1** using the Bader's theory of "atoms in molecules" (AIM).[29] The existence of a bond critical point and bond path connecting two atoms is an unambiguous evidence of interaction. In Fig. 8c we show the AIM analysis of the dimer of compound **1** and it can be observed that the antiparallel π–π interaction is characterized by the presence of two bond critical points (green spheres) that interconnect two atoms of the pyridine rings, thus confirming the interaction. Furthermore, the distribution of critical points reveals the existence of two symmetrically related C–H···N and C–H···S H-bonding interactions since two bond critical points connect the N and S atoms of the pseudohalide with the aromatic H-atoms. A ring critical point (yellow sphere) also appears upon complexation due to the formation of a supramolecular ring.

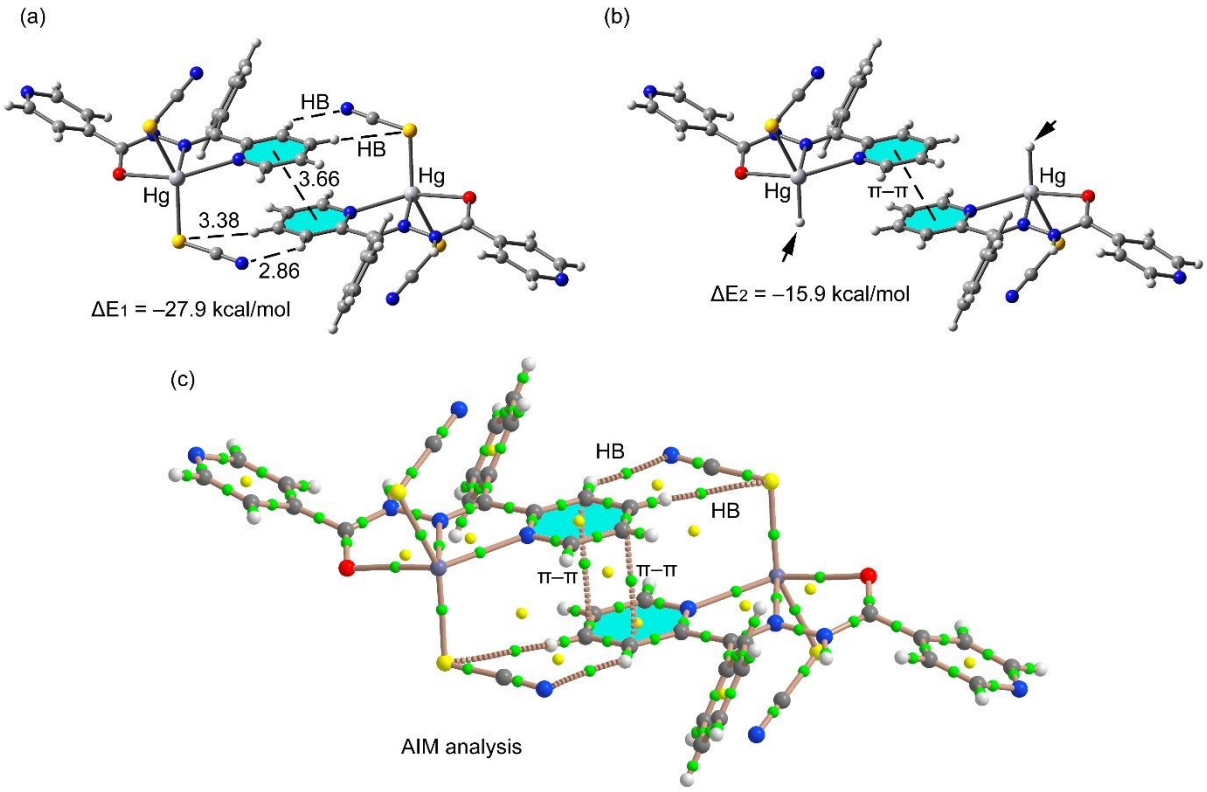

Published on 30 October 2018. Downloaded by University of Strathclyde on 10/31/2018 6:29:35 PM.

CrystEngComm Accepted Manuscript

View Article Online
DOI: 10.1039/C8CE01580E

Fig. 8. (a) Interaction energy of the self-assembled π-stacked dimer observed in the solid state of compound **1**. Distances in Å. (b) Interaction energy in the theoretical model of **1**. (c) AIM an analysis of the self-assembled dimer retrieved from the X-ray structure of compound **1**. Bond and ring critical points are represented by green and yellow spheres, respectively. The bond paths connecting bond critical points are also represented by dashed lines.

In compound **2** we have computed the interaction energy of the self-assembled π–stacked dimer shown in Fig. 9a, which is stabilized by an intricate combination of noncovalent interactions. That is, H-bonds (red dashed lines), π–π stacking interactions between the coordinated and uncoordinated pyridine rings and chelate ring···chelate ring (CR–CR) stacking interactions. Remarkably, opposite to compound **1**, the square planar pyramidal geometry of the Hg atom in compound **2** facilitates the approximation of the chelate rings, resulting in shorter CR···CR interactions (3.54 Å). The dimerization energy (ΔE_3 = –64.6 kcal/mol) is very large due to the contribution of the three interactions and the strong dipole···dipole interactions due to the zwitterionic nature of the ligand. In an effort to roughly estimate the contribution of the different forces that govern the formation of the self-assembled dimer, we have computed a theoretical model in which the methyl groups have been replaced by H atoms (see small arrows in Fig. 9b) and consequently the C–H···S H–bonds involving the methyl groups are not formed. As a result, the interaction energy is reduced to ΔE_4 = –57.6. Therefore, the contribution of both symmetrically equivalent H-bond can be estimated by difference (–7 kcal/mol). Furthermore, we have used an additional dimer, where the pyridinium ring has been replaced by a hydrogen atom, and consequently, the py···py interactions and H-bonds are not formed. Since the pyridine rings are protonated, in this model we have added a hydrogen atom to the hydrazone group to keep the model neutral. The resulting interaction energy is further reduced to ΔE_5 = –30.5 kcal/mol kcal/mol which corresponds to the contribution of the CR–CR π–stacking interaction. The contribution of both py···py interactions and C–H···S bonds can be estimated by difference (–27.1 kcal/mol) thus emphasizing the importance of these charge-assisted π-stacking interactions. The CR–CR interaction is unexpectedly strong, which is likely due to the model used for the calculations where an H-atom has been added to the hydrazone group. This H-atoms likely forms an extra H-bond with the S atom of the pseudohalide ligand, thus also contributing to the binding energy (see blue dashed line in Fig. 9c). Therefore, the conventional py···py interaction is underestimated and the CR–CR interaction is overestimated using this model. Nevertheless, the strong binding energy of the whole assembly indicates that this

Published on 30 October 2018. Downloaded by University of Strathclyde on 10/31/2018 6:29:35 PM.

CrystEngComm Accepted Manuscript

View Article Online
DOI: 10.1039/C8CE01580E

combination of two types of π-stacking interactions and H-bonds is a robust binding motif in the solid state of compound **2**.

In Fig. 9d we show the AIM analysis of compound **2**. Each conventional π–π interaction (pyridine rings) is characterized by the presence of two bond critical points that interconnect two atoms of the protonated pyridine ring to two atoms of the coordinated one, thus confirming the interaction. Furthermore, the distribution of critical points reveals the existence of four symmetrically related C–H···S H-bonding interactions. Each one is characterized by a bond critical point and bond path connecting the H atom with the S atom of the pseudohalide. Finally, the unconventional CR···CR interaction is confirmed by the presence of two bond critical points interconnecting the Hg atoms to the N atoms and two additional bond critical points connecting the O atoms to the C atoms of the hydrazone group. The value of the Laplacian of the charge density at the bond critical points is positive, as is common in closed-shell interactions.

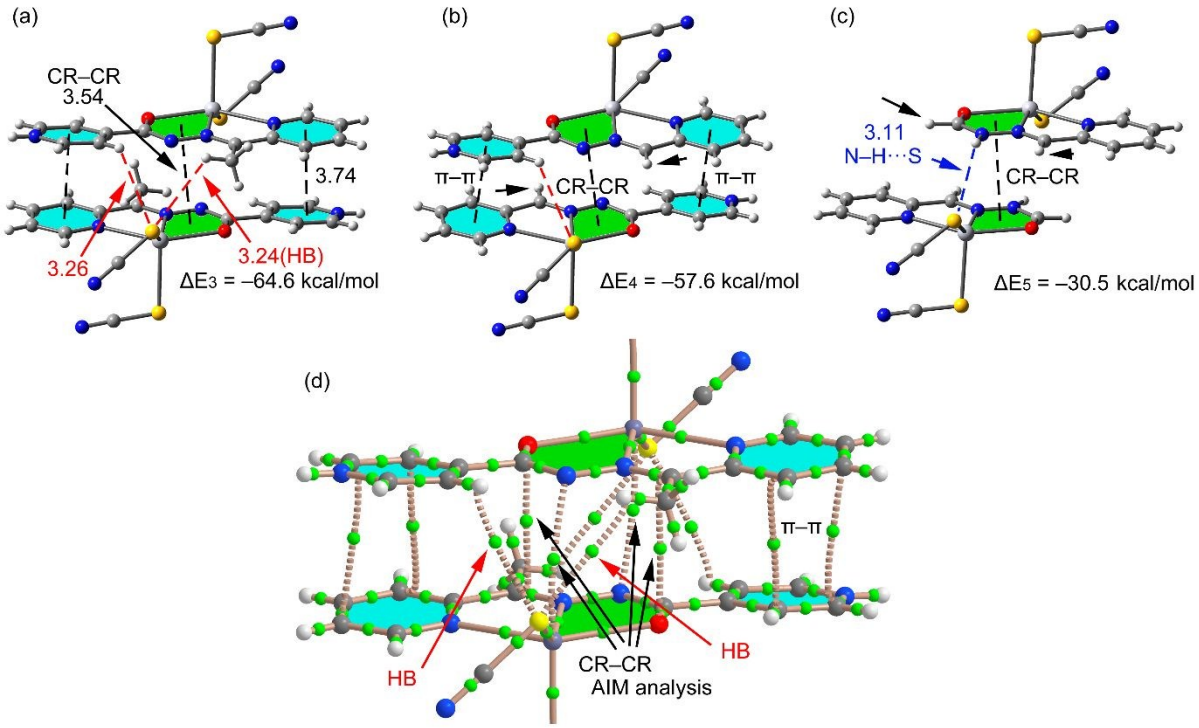

Fig. 9. (a) Interaction energy of the self-assembled π-stacked dimer observed in the solid state of compound **2**. Distances in Å. (b-c) Geometries and interaction energies in the theoretical models of **2**. (c) AIM an analysis of the self-assembled dimer retrieved from the X-ray structure of compound **1**. Bond critical points are represented by green spheres. The bond paths

Published on 30 October 2018. Downloaded by University of Strathclyde on 10/31/2018 6:29:35 PM.

CrystEngComm Accepted Manuscript

View Article Online
DOI: 10.1039/C8CE01580E

connecting bond critical points are also represented by dashed lines. Ring and cage critical points have been omitted for clarity

The binding energies and π-stacking distances (3.54 Å) described above for the CR···CR interactions in compound **2** are comparable to those reported for Hg(II) complexes where halide instead of pseudohalides were used as co-ligands (3.30 to 3.67 Å).[30] CR···CR interactions have been also described recently in Zn(II) and Cd(II) complexes involving (iso)nicotinohydrazide ligands that exhibited similar binding energies (~–28 kcal/mol) and distances (3.44-3.50 Å).[13a] Moreover, a recent study has described CR···CR interactions in Cu(II) polymers where polydentate (*E*)—2–(1–(pyridin–2–yl)–methyleneamino)–terephthalic acid was used as ligand.[31] The solid state X-ray architecture of the polymers was governed by CR···CR interactions along with H-bonding. These reports along with the structures reported herein provide strong evidence for preferential formation of chelate ring stackings, which can be considered as a synthon interaction for (iso)nicotinohydrazide metal complexes. Moreover, the interaction energies reported herein confirm that the chelate–chelate interactions are stronger than those reported for classical π–π complexes.[28]

Conclusions

Herein, we reported the syntheses and characterization of two mercury(II) complexes of two isonicotinohydrazone Schiff base ligands. The ligands acted as pincer type tridentate N_2O-donor ligands, in which the isonicotinamide pyridine nitrogen remained uncoordinated. By using thiocyanate ligands along with the organic ligands, the coordination geometry around each mercury center resulted in distorted trigonal bipyramid and square-pyramid in **1** and **2**, respectively. Compounds **1** and **2** exhibit interesting π-π stacking interactions in their solid state, which have been analyzed using DFT calculations in detail. The combination of conventional π-stacking with more unconventional chelate ring stacking interactions is a robust binding motif in compound **2**. The protonation of 4-pyridyl substituent may increase the strength of the pincer type coordination in hydrazone based Schiff base ligands. The presented systems are complementary in the sense of proton donor and proton acceptor properties of the molecular subcomponents. The proton transfer should not be overlooked when designing new structures based on supplementary molecular fragments such as hydrazone based ligands substituted with pyridines. It should be emphasized that steric effects (bulky phenyl vs methyl) is the origin for the different behaviour of the complexes. The proton transfer in isonicotinohydrazone methyl substituted ligand (HL^2) enables the intramolecular coupling and flattening of the molecule

Published on 30 October 2018. Downloaded by University of Strathclyde on 10/31/2018 6:29:35 PM.

CrystEngComm Accepted Manuscript

View Article Online
DOI: 10.1039/C8CE01580E

which increases the chances for stronger pincer type coordination. It favors the conventional (π–π) and unconventional chelate ring stacking interactions, which are useful tools in crystal engineering.

Acknowledgements

We are grateful to the University of Maragheh for the financial support of this research. The publication was also prepared with the support of the "RUDN University Program 5-100". AF thanks the MINECO/AEI from Spain for a "Juan de la Cierva" contract. We thank the MINECO/AEI from Spain for financial support (project number CTQ2017-85821-R, FEDER funds). We are grateful to the CTI (UIB) for free allocation of computer time.

References

1 M. O. Besenhard, P. Neugebauer, O. Scheibelhofer and J. G. Khinast, *Cryst. Growth Des.*, 2017, **17**, 6432.

2 P. Erk, H. Hengelsberg, M. F. Haddow and R. van Gelder, *CrystEngComm*, 2004, **6**, 474.

3 N. Tumanova, N. Tumanov, K. Robeyns, F. Fischer, L. Fusaro, F. Morelle, V. Ban, G. Hautier, Y. Filinchuk, J. Wouters, T. Leyssens and F. Emmerling, *Cryst. Growth Des.*, 2018, **18**, 954.

4 J. R. G. Sander, D.-K. Bučar, R. F. Henry, B. N. Giangiorgi, G. G. Z. Zhang and L. R. MacGillivray, *CrystEngComm*, 2013, **15**, 4816.

5 D.-K. Bučar, *Cryst. Growth Des.*, 2017, **17**, 2913.

6 G. R. Desiraju, *J. Am. Chem. Soc.*, 2013, **135**, 9952.

7 A. J. Blake, N. R. Champness, P. Hubberstey, W-S. Li, M. A.Withersby and M. Schröder, *Coord. Chem. Rev.*, 1999, **183**, 117.

8 M. Sarkar and K. Biradha, *Cryst. Growth Des.*, 2007, **7**, 1318.

9 A. Beheshti, W. Clegg, V. Nobakht and R. W. Harrington, *Cryst. Growth Des.*, 2013,

Published on 30 October 2018. Downloaded by University of Strathclyde on 10/31/2018 6:29:35 PM.

CrystEngComm Accepted Manuscript

View Article Online
DOI: 10.1039/C8CE01580E

Published on 30 October 2018. Downloaded by University of Strathclyde on 10/31/2018 6:29:35 PM.

13, 1023.

10 K. J. Szabó and O. F. Wendt, "Pincer and Pincer-Type Complexes: Applications in Organic Synthesis and Catalysis.," by John Wiley & Sons, Inc.

11 (a) S. Yumnam and L. Rajkumari, *J. Chem. Eng. Data*., 2009, **54**, 28; (b) A. A. Khandar, B. K. Ghosh, C. Lampropoulos, M. S. Gargari, V. T. Yilmaz, K. Bhar, S. A. Hosseini-Yazdi, J. M. Cain and G. Mahmoudi, *Polyhedron*, 2015, **85**, 467. (c) M. Abedi, O. Z. Yesilel, G. Mahmoudi, A. Bauza, S. E. Lofland, Y. Yerli, W. Kaminsky, P. Garczarek, J. K. Zareba, A. Ienco, A. Frontera and M. S. Gargari, *Inorg. Chim. Acta.*, 2016, **443**, 101; (d) G. Mahmoudi, A. Bauzá, A. V. Gurbanov, F. I. Zubkov, W. Maniukiewicz, A. Rodríguez-Diéguez, E. López-Torres and A. Frontera, *CrystEngComm*, 2016, **18**, 9056; (e) M. S. Gargari, V. Stilinovic´, A. Bauzá and A. Frontera, *Chem. Eur. J*., 2015, **21**, 17951.

12 (a) M. Fujita, D. Oguro, M. Miyazawa, H. Oka, K. Yamaguchi, K. Ogura, *Nature*, 1995, **378**, 469; (b) J. Xie, S. Shen, R. Chen, J. Xu, K. Dong, J. Huang, Qin Lu, Wenjiao Zhu, Tieliang Ma, L. Jia, H. Cai and T. Zhu, *Org Lett*. 2017, **13**, 4413–4419; (c) Z. Y. Hao, Q. W. Liu, J. Xu, L. Jia and S. B. Li, *Chem. Pharm. Bull*., 2010, **58**, 1306–1312.

13 (a) G. Mahmoudi, J. K. Zaręba, A. Bauza, M. Kubicki, A. Bartyzel, A. Keramidas, L. Butusov, B. Miroslaw and A. Frontera, *CrystEngComm*, 2018, **20**, 1065; (b) A. A. Khandar, F. A. Afkhami, S. A. Hosseini-Yazdi, J. M. White, S. Kassel, W. G. Dougherty, J. Lipkowski, D. Van Derveer, G. Giester and F. Costantino, *Inorg. Chim. Acta*, 2015, **427**, 87; (c) A. A. Khandar, F. A. Afkhami, S. A. Hosseini-Yazdi, J. Lipkowski, W. G. Dougherty, W. S. Kassel, H. R. Prieto and S. G. Granda, *J. Inorg. Organomet. Polym*. 2015, **25**, 860; (d) F. A. Afkhami, A. A. Khandar, J. M. White, A. Guerri, A. Ienco, J. T. Bryant, N. Mhesn and C. Lampropoulos, *Inorg. Chim. Acta*, 2017, **457**, 150; (e) F. A. Afkhami, A. A. Khandar, G. Mahmoudi, M. Amini, E. Molins, P. Garczarek, J. Lipkowski, J. M. White and A. M. Kirillov, *Inorg. Chim. Acta*, 2017, **458**, 68; (f) D. Hean, T. Gelbrich, U. J. Griesser, J. P. Michael and A. Lemmerer, *CrystEngComm*, 2015, **17**, 5143-5153; (g) J. A. Lessa, G. L. Parrilha, H. Beraldo, *Inorg. Chim. Acta*, 2012, **393**, 53–63; (h) G. N. Babu, A. R. B. Rao, S. Keesara and S. Pal, *J. Organomet. Chem*., 2017, **848**, 243; (i) P. Doungdee, S. Sarel, N. Wongvisetsirikul and S. Avramovici-Grisaru, *J. Chem. Soc. Perkin Trans. 2*,1995, 319

CrystEngComm Accepted Manuscript

View Article Online
DOI: 10.1039/C8CE01580E

14 (a) S. Yumnam and L. Rajkumari, *J. Chem. Eng. Data*. 2009, **54**, 28; (b) C. M. Armstrong, P. V. Bernhardt, P. Chin and D. R. Richardson, *Eur. J. Inorg. Chem*. 2003, 1145; (c) C. B. Aakeröy, S. Forbes and J. Desper, *CrystEngComm* 2012, **14**, 2435; (d) Z. He, C. He, E. Q. Gao, Z. M. Wang, X. F. Yang, C. S. Liao and C. H. Yan, *Inorg. Chem. 2003,* **42**, 2206; (e) K. L. Abboud, R. C. Palenik, G. J. Palenik and R. M. Wood, *Inorg. Chim. Acta*. 2007, **360**, 3642; (f) F. A. Afkhami, A. Akbar Khandar, G. Mahmoudi, W. Maniukiewicz, J. Lipkowski, J. M. White, R. Waterman, S. G-, Granda, E. Zangrando, A. Bauzái and A. Frontera, *CrystEngComm*, 2016, **18**, 4587.

15 "Crystal Explorer package." ver. 3.1 S. K. Wolff, D. J. Grimwood, J. J. McKinnon, M. J. Turner, D. Jayatilaka and M. A. Spackman, Crystal Explorer ver. 3.1, University of Western Australia, Perth, Australia, 2013.

16 "SAINT Plus." Data Reduction and Correction Program, v. 6.01, Bruker AXS, Madison, Wisconsin, USA, 1998.

17 "SADABS." v.2.01, Bruker/Siemens Area Detector Absorption Correction Program, Bruker AXS, Madison, Wisconsin, USA, 1998.

18 G. M. Sheldrick, *Acta Crystallogr. Sect. C Struct. Chem.*, 2015, **71**.

19 O. V. Dolomanov, L. J. Bourhis, R. J. Gildea, J. A. K. Howard and H. Puschmann, *J. Appl. Crystallogr.*, 2009, **42**, 339.

20 M. J. Frisch, G. W. Trucks, H. B. Schlegel, G. E. Scuseria, M. A. Robb, J. R. Cheeseman, G. Scalmani, V. Barone, B. Mennucci, G. A. Petersson, H. Nakatsuji, M. Caricato, X. Li, H. P. Hratchian, A. F. Izmaylov, J. Bloino, G. Zheng, J. L. Sonnenberg, M. Hada, M. Ehara, K. Toyota, R. Fukuda, J. Hasegawa, M. Ishida, T. Nakajima, Y. Honda, O. Kitao, H. Nakai, T. Vreven, J. A. Montgomery, Jr., J. E. Peralta, F. Ogliaro, M. Bearpark, J. J. Heyd, E. Brothers, K. N. Kudin, V. N. Staroverov, R. Kobayashi, J. Normand, K. Raghavachari, A. Rendell, J. C. Burant, S. S. Iyengar, J. Tomasi, M. Cossi, N. Rega, J. M. Millam, M. Klene, J. E. Knox, J. B. Cross, V. Bakken, C. Adamo, J. Jaramillo, R. Gomperts, R. E. Stratmann, O. Yazyev, A. J. Austin, R. Cammi, C. Pomelli, J. W. Ochterski, R. L. Martin, K. Morokuma, V. G. Zakrzewski, G. A. Voth, P. Salvador, J. J. Dannenberg, S. Dapprich, A. D. Daniels, Ö. Farkas, J. B. Foresman, J. V. Ortiz, J. Cioslowski, and D. J. Fox, Gaussian 09 (Gaussian, Inc., Wallingford CT, 2009).

Published on 30 October 2018. Downloaded by University of Strathclyde on 10/31/2018 6:29:35 PM.

CrystEngComm Accepted Manuscript

View Article Online
DOI: 10.1039/C8CE01580E

Published on 30 October 2018. Downloaded by University of Strathclyde on 10/31/2018 6:29:35 PM.

21 S. F. Boys and F. Bernardi, *Mol. Phys.*, 1970, **19**, 553–566.

22 R. F. W. Bader, *Chem. Rev.*, 1991, **91**, 893–928.

23 T. A. Keith, AIMAll (Version 13.05.06), TK Gristmill Software, Overland Park KS, USA, 2013.

24 T.-F. Zhu, R.-H. Chen, T.-L. Ma, Y. Wang and Z.-Q. Xu, *Transition Met. Chem*., 2015, **40**, 485.

25 J. J. McKinnon, D. Jayatilaka and M. A. Spackman, *Chem. Commun.*, 2007, 3814.

26 M. A. Spackman and D. Jayatilaka, *CrystEngComm*, 2009, **11**, 19.

27 (a) B. D. Ostojić, G. V. Janjić and S. D. Zarić, *Chem. Commun.*, 2008, **48**, 6546-6548; (b) Z. D. Tomić, S. B. Novaković and S. D. Zarić, *Eur. J. Inorg. Chem.*, 2004, **11**, 2215-2218; (c) D. N. Sredojević, Z. D. Tomić and S. D. Zarić, *Cent. Eur. J. Chem.*, 2007, **5**, 20-31; d) Z. D. Tomić, D. N. Sredojević and S. D. Zarić, *Cryst. Growth Des.*, 2006, **6**, 29-31; (e) D. N. Sredojević, G. A. Bogdanović, Z. D. Tomić and S. D. Zarić, *CrystEngComm*, 2007, 9, 793-798; (f) A. Castineiras, A. G. Sicilia-Zafra, J. M. Gonzales-Perez, D. Choquesillo-Lazarte and J. Niclos-Gutierrez, *Inorg. Chem.*, 2002, **41**, 6956-6958; (g) E. Craven, C. Zhang, C. Janiak, G. Rheinwald and H. Lang, *Z. Anorg. Allg. Chem.*, 2003, **629**, 2282-2290; (h) U. Mukhopadhyay, D. Choquesillo-Lazarte, J. Niclos-Gutierrez and I. Bernal, *CrystEngComm*, 2004, 6, 627-632; (i) D. Pucci, V. Albertini, R. Bloise, A. Bellusci, A. Cataldi, C. V. Catapano, M. Ghedini and A. Crispini, *J. Inorg. Biochem.*, 2006, **100**, 1575-1578; (j) S. P. Mosae, E. Suresh and P. S. Subramanian, *Polyhedron*, 2009, **28**, 245-252; (k) X. J. Wang, H. X. Jian, Z. P. Liu, Q. L. Ni, L. C. Gui and L. H. Tang, *Polyhedron*, 2008, **27**, 2634-2642; (l) S. Chowdhury, M. G. B. Drew and D. Datta*, Inorg. Chem. Commun*., 2003, **6**, 1014-1016; (m) X. Wang, O. V. Sarycheva, B. D. Koivisto, A. H. McKie and F. Hof, *Org. Lett.*, 2008, **100**, 297-300.

28 (a) A. K. Tewari and R. Dubey, *Bioorg. Med. Chem.*, 2008, **16**, 126-143; (b) P. Mignon, S. Loverix, J. Steyaert and P. Geerlings, *Nucleic Acids Res.*, 2005, **33**, 1779-1789; (c) J. Sponer, K.E. Riley and P. Hobza, *Phys. Chem. Chem. Phys.*, 2008, **10**, 2595-2610; (d) X. J. Wang, L. C. Gui, Q. L. Ni, Y. F. Liao, X.F. Jiang, L. H. Tang, L. H. Zhang and Q. Wu, *CrystEngComm,* 2008, **10**, 1003-1010; (e) S. L. Cockroft, C. A. Hunter, K. R.

CrystEngComm Accepted Manuscript

View Article Online
DOI: 10.1039/C8CE01580E

Lawson, J. Perkins and C. J. Urch, *J. Am. Chem. Soc.*, 2005, **127**, 8594-8595; (f) T. Sato, T. Tsuneda and K. Hirao, *J. Chem. Phys.*, 2005, **123**, 104307-104317; (g) S. Grimme, *Angew. Chem. Int. Ed.*, 2008, **47**, 3430-3434; (h) M. Rubeš, O. Bludsky' and P. Nachtigall, *ChemPhysChem*, 2008, 9, 1702-1708; (i) E. C. Lee, D. Kim, P. Jurecka, P. Tarakeshwar, P. Hobza and K. S. Kim, *J. Phys. Chem. A*, 2007, **111**, 3446-3457; (j) M. O. Sinnokrot and C.D. Sherrill, *J. Phys. Chem. A*, 2006, **110**, 1065610668; (k) R. Podeszwa, R. Bukowski and K. Szalewicz, *J. Phys. Chem. A*, 2006, **110**, 10345-10354; (l) M. Pitonak, P. Neogrady, J. Rezac, P. Jurecka, M. Urban and P. Hobza, *J. Chem. Theory Comput.*, 2008, **4**, 1829-1834.

29 R. F. W. Bader, *J. Phys. Chem. A*, 1998, **102**, 7314–7323.

30 F. A. Afkhami, A. A. Khandar, G. Mahmoudi, W. Maniukiewicz, A. V. Gurbanov, F. I. Zubkov, O. Sahin, O. Z. Yesilel and A. Frontera, *CrystEngComm*, 2017, **19**, 1389.

31. S. Saha, N. Biswas, A. Sasmal, C. J. Gómez-García, E. Garribba, A. Bauza, A. Frontera, G. Pilet, G. M. Rosair, S. Mitra and C. Roy Choudhury, *Dalton Trans*, 2018, DOI: 10.1039/C8DT02417K.

Published on 30 October 2018. Downloaded by University of Strathclyde on 10/31/2018 6:29:35 PM.

CrystEngComm Accepted Manuscript

View Article Online
DOI: 10.1039/C8CE01580E

We report the synthesis and X-ray characterization and theoretical study of two Hg(II) complexes with pincer-type isonicotinohydrazone Schiff base ligands to analyze chelate-ring π-stacked assemblies

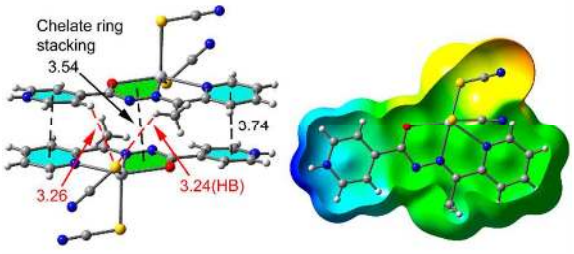

Published on 30 October 2018. Downloaded by University of Strathclyde on 10/31/2018 6:29:35 PM.

CrystEngComm Accepted Manuscript